Simulation and theory of temperature gradient driven turbulence

F. Jenko, W. Dorland*, B. Scott, D. Strintzi

Max-Planck-Institut für Plasmaphysik, EURATOM Association, Boltzmannstr. 2, 85748 Garching, Germany

Neglecting Debye screening effects, ion and electron temperature gradient (ITG/ETG) modes are isomorphic in the electrostatic and adiabatic limit. Therefore linear results obtained for one of these microinstabilities can also be applied to the other one by simply interchanging the species labels. In the nonlinear regime, this symmetry is broken, however. Mode saturation is caused by two distinct secondary instabilities, one of which depends on the details of the adiabatic response and therefore differs for ITG and ETG modes. This effect allows for the formation of high-amplitude streamers in the ETG case, raising the transport levels way beyond mixing length estimates. The turbulent transport arising from this competition between linear streamers and secondary instabilities is predicted well by an *ab initio* numerical model as long as self-generated zonal flows and fields do not back-react on the turbulent dynamics. A successful attempt to condense several important pieces of information about the saturated nonlinear state into simple algebraic formulas will be presented. It raises the hope that it might indeed be possible to construct a useful analytic theory of temperature gradient driven turbulence and transport in fusion plasmas.

I. ARE ITG AND ETG TURBULENCE ISOMORPHIC?

For $\lambda_{De} \lesssim \rho_e$, ITG and ETG modes are perfectly isomorphic in the electrostatic and adiabatic regime which we will mainly focus on in the present paper. Under these

*IREAP, University of Maryland, College Park, Maryland 20742, USA

circumstances, it is therefore permissible to transfer linear results from one field of study to the other one by simply interchanging the species labels. In the nonlinear regime, this symmetry is broken, however. And at the heart of this asymmetry lies a subtle difference in the response of the adiabatic species. [1] In the ITG case, electron adiabaticity is caused by fast parallel motion, $k_\parallel v_{te} \gg \omega$, leading to an Ohm's law of the form $\nabla_\parallel(\tilde{n}_e/n_{e0} - e\tilde{\phi}/T_{e0}) = 0$. Therefore the ratio $\tilde{n}_e/\tilde{\phi}$ is only constant up to an arbitrary function of the flux surface label. The resulting adiabaticity equation may be written as

$$\frac{\tilde{n}_e}{n_{e0}} = \frac{e\,(\tilde{\phi} - \langle\langle\tilde{\phi}\rangle\rangle)}{T_{e0}} \tag{1}$$

where double angular brackets denote flux-surface averaging. Eq. (1) means that density fluctuations do not respond to potential fluctuations which are constant on flux surfaces. In the ETG case, on the other hand, ion adiabaticity follows from the fact that the ion gyroradii are large compared to the typical perpendicular wavelengths of ETG modes, $k_\perp \rho_i \gg 1$. In this limit, the gyrokinetic Poisson equation reads

$$\frac{\tilde{n}_i}{n_{i0}} = -\frac{e\tilde{\phi}}{T_{i0}}\,. \tag{2}$$

This form of adiabaticity is caused by perpendicular rather than by parallel motion, shielding zonal (i.e., purely radially varying) components of $\tilde{\phi}$.

Although the difference between Eqs. (1) and (2) has no effect on linear ITG/ETG modes, it may strongly affect their nonlinear dynamics via the mechanisms leading to turbulent saturation as is demonstrated in Fig. 1. The physical parameters in these nonlinear gyrokinetic simulations are $L_n/R = 1$ ($L_n/R = 0$ for the slab runs), $L_n/L_T = 10$, $q = 2$, $\hat{s} = 0.5$, and $T_{e0}/T_{i0} = 1$. The normalization is conventional: the heat fluxes are normalized to $p_{0j}v_{tj}(\rho_j/L_n)^2$, where ρ_j is the gyroradius of thermal ions or electrons (in the ITG and ETG cases, respectively), v_{tj} is the thermal velocity of the ions or electrons, respectively, and p_{0j} is the background pressure of the jth species. Similarly, the time is normalized to v_{tj}/L_n. Some main features of Fig. 1 can be described as follows. (1) In the sheared slab cases, the ETG and ITG simulations saturate at similar normalized levels consistent with mixing length expectations, $\chi \sim \gamma^{\max}/k_\theta^2 \sim \rho^2 v_t/L_T$. (2) In the cases labeled 'Curv', we set the curvature to a constant value characteristic of the curvature at the outboard midplane of a conventional tokamak. The ETG

simulation now goes to much higher normalized amplitude than its ITG counterpart and exhibits streamers. How can this type of behavior be interpreted? Since the ETG and ITG simulations differ only in the details of the adiabatic species' response (leaving linear mode properties invariant), we will have to explore the physics of nonlinear saturation. This will be done in the conceptual framework of secondary instability theory.

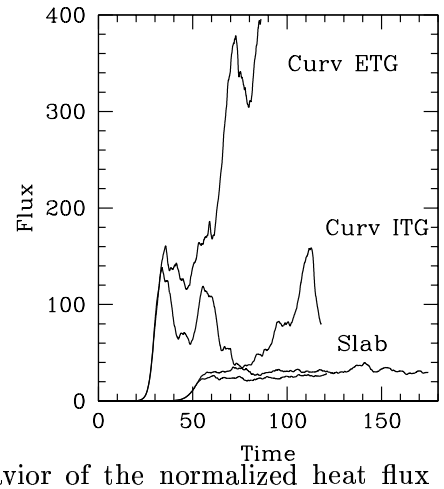

FIG. 1. Qualitative behavior of the normalized heat flux as the adiabatic response is changed (ETG *vs.* ITG), and as the instability drive is changed ("Slab" *vs.* "Curv").

Depending on the degree of "slabness" (as characterized by the intrinsic parallel velocity component) of linear electrostatic ETG/ITG modes, we find that one of two distinct processes may dominate as nonlinear saturation mechanism. [2] Perpendicular shear in the *parallel* flow of the linear instability drives a strong (hereafter, "Cowley") secondary, described in detail in Ref. [3]. Importantly, this secondary is not sensitive to the form of the adiabatic response and thus leads to the same (mixing-length type) transport level in both slab cases. Predominatly curvature driven modes, on the other hand, are broken up by a secondary (hereafter, "Rogers") instability that is driven by the perpendicular shear in the eigenmode's *perpendicular* $\mathbf{E} \times \mathbf{B}$ flow. [1,4] Because the Rogers secondary is significantly weakened on ρ_e scales (as compared to ρ_i scales) by the adiabatic ion response, a curvature driven ETG mode tends to saturate at a much higher normalized level than both its ITG counterpart and mixing length expectations. With this enhancement, associated with high-amplitude streamers, ETG-induced transport can be comparable to electron energy transport induced by ITG modes and trapped electron modes.

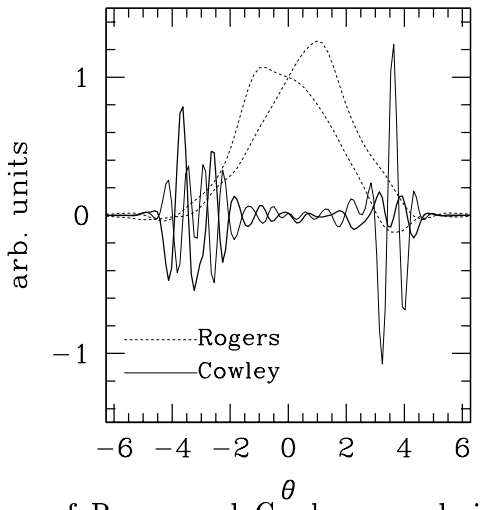

FIG. 2. Typical structures of Rogers and Cowley secondaries along the field line for $k_y\rho_e = 0.2$ and $k_x = k_y/2$ component of predominantly curvature-driven and slab-like primaries, respectively.

Another key difference between these two types of secondaries can be visualized as follows. Freezing a given linear ETG/ITG streamer at a high amplitude (thereby reducing complications arising from the formally linear terms) and using this state as the "equilibrium" for an instability calculation, we obtain parallel mode structures like the ones shown in Fig. 2. Whereas the Rogers secondary is localized to the maximum of the shear in the perpendicular flow (in this case, near $\theta = 0$) and has a small parallel wavenumber (with constant curvature, $k_{||} = 0$), the Cowley secondary is localized to the region where there is a finite poloidal gradient of the parallel velocity and zero perpendicular velocity, and has a large parallel wavenumber that is directly proportional to the amplitude of the primary. Let us note in passing that the k_x spectra (not shown) of Cowley and Rogers secondaries are also very different. The Rogers secondary has a cut-off at $k_x/k_y = 1$, while the Cowley secondary extends to high k_x/k_y. Here, k_y is the poloidal wavenumber of the linear ITG/ETG streamer.

Thus, we have demonstrated that in the framework of secondary instability theory, it is possible to explain the qualitative features of our simulation results shown in Fig. 1. In the remainder of this paper, we will try to capitalize on the insight gained so far and to use it as a guiding principle for quantitative semi-analytical predictions of ETG/ITG driven turbulence and transport. We will study the ETG case first and in more detail.

II. ON THE CHARACTER OF ETG TURBULENCE AND TRANSPORT

To study the behavior of toroidal ETG turbulence for realistic conditions, we use two independently developed codes, `gene` and `gs2` (for a description of both codes, see Ref. [1] and references therein), to solve the nonlinear electromagnetic gyrokinetic Vlasov-Maxwell equations [5,6] in magnetic flux-tube geometry [3,7] employing a fixed grid in five-dimensional phase space. Various simulation results have been published in previous papers [1,2,4,8–10] and shall only be briefly summarized and commented here. This overview will help to draw the contours of a picture of ETG turbulence which we will then try to cast into a semi-analytical form.

On the nature of high-amplitude streamers. The single most striking feature in nonlinear ETG simulations is the occurrence of radially elongated vortices with large fluctuation amplitudes in certain parameter regimes. [1] Because of the low intrinsic mixing length level for ETG modes, the presence of high-amplitude streamers is vital in order to achieve experimentally relevant values of the electron heat conductivity χ_e. Streamers have been observed both in tokamak [1,2,4] and in stellarator [9,10] simulations if and only if the underlying long-wavelength instabilities have a clear toroidal (*vs.* slab) character. For large aspect ratio tokamaks with circular cross section and small Shafranov shift, this is the case for $\hat{s} \gtrsim 0.4$ and $R/L_{T_e} \gg R/L_{T_e}^{\mathrm{crit}}$. [1] In the presence of streamers, the fluctuation and transport levels can be boosted by more than an order of magnitude with respect to mixing length expectations. Streamer aspect ratios computed via the radial/poloidal autocorrelation functions of $\tilde{\phi}$ are typically of the order of 2. [10] This value seems a little low compared with one's visual impression and might indicate that refined measurements are called for (i.e., inspired by percolation theory). The dominant modes for Cyclone base case parameters have $k_\theta \rho_e \sim 0.15$ [1,2] and exibit a phase shift of $\sim \pi/3$ between $\tilde{\phi}$ and $\tilde{T}$ (which is basically equal to that of the corresponding linear streamer). [1] At higher values of k_θ, the spectra exhibit a power law behavior with exponents that seem to be quite universal. [2,10] The turbulent transport (both with *and* without streamers) is always predominantly electrostatic. [1,9]

Some of these qualitative features may be reproduced with a very simple two dimensional gyrofluid model. For this, the ions are assumed to be adiabatic and finite ρ_e

effects are neglected except for the screening which provides the finite vorticity. The electrons are described by the following two moment model,

$$\partial_t \tilde{n}_e = -\mathbf{v}_E \cdot \nabla \tilde{n}_e + D\left(\tilde{\phi} - \tilde{n}_e - 1.71\,\tilde{T}_e\right) + \omega_B\,\partial_y\left(\tilde{\phi} - \tilde{n}_e - \tilde{T}_e\right), \tag{3}$$

$$\partial_t \tilde{T}_e = -\mathbf{v}_E \cdot \nabla(\tilde{T}_e - x) + D\left(1.71\,(\tilde{\phi} - \tilde{n}_e) - 4.52\,\tilde{T}_e\right) + \omega_B\,\partial_y\left(\tilde{\phi} - \tilde{n}_e - 2.5\,\tilde{T}_e\right), \tag{4}$$

with the polarization given by

$$\left(\tau_e - \mu_e \nabla_\perp^2\right)\tilde{\phi} = -\tilde{n}_e \tag{5}$$

where $\omega_B = 2L_{T_e}/R$ and $\mu_e = m_e/m_i$. The dependent variables, $\tilde{\phi}$, $\tilde{n}_e$, and $\tilde{T}_e$, are relative fluctuation levels in terms of T_{e0}/e, n_{e0}, and T_{e0}, normalized with an additional factor of $\delta = \rho_s/L_{T_e}$. Normalization of time and space scales follows c_s/L_{T_e} and ρ_s, respectively. The spatial domain, (x, y) is the drift plane, with the parallel dynamics modelled through the dissipative coupling coefficient, D, whose nominal value is $L_{T_e} k_\parallel v_{te}/c_s$. The spatial grid is 256^2 nodes on a domain of $(4\pi\rho_s/3)^2$, and the timestep is 0.001 in these ITG units, though the scales are those of ETG turbulence. The typical result is exemplified for $D = 1$, $\omega_B = 0.2$, $\mu_e = 1/3670$, and $\tau_e = 1$, run to $t = 25$. Saturation occurs by $t = 10$ and statistical measurements are taken over $10 < t < 25$. The electron thermal transport is quite substantial, $\chi_e = (0.29 \pm 0.03)\,\rho_s^2 c_s/L_{T_e} = (17.6 \pm 1.8)\,\rho_e^2 v_{te}/L_{T_e}$. The correlation lengths in x and y are $0.19\rho_s$ $(11.5\rho_e)$ and $0.10\rho_s$ $(6.1\rho_e)$, respectively, indicative of streamer activity. These appear prominently in the spatial morphology of both $\tilde{n}_e$ and $\tilde{T}_e$. The spectrum is relatively broadband, with the transport peak near $k_y\rho_s = 10$ $(k_y\rho_e \sim 0.16)$ set by the parallel dissipation. Most important in the context of this study is an energetic analysis of Eqs. (3-5) similar to that of a drift wave system [11]. The time evolution of the $\mathbf{E}\times\mathbf{B}$ energy, $E_e = \int dV\,[(\tau_e + \mu_e k_\perp^2)\,\tilde{\phi}^2/2]$, can be written as $\partial_t E_e = \mathrm{Tr}_e - \mathrm{Tr}_j + \mathrm{Tr}_p$. The three terms describing nonlinear redistribution, parallel dissipation, and interchange forcing correspond to the three terms on the RHS of Eq. (3) and are Fourier decomposed in (k_x, k_y) space. We find that the interchange forcing is closely balanced by the dissipation, with the nonlinear effects being very subdominant (see Fig 3). Both linear signals are found to peak on the $k_x = 0$ axis. This is a decisive signal for the linear

drive of and energetic dominance by the streamers, in accordance with the findings in gyrokinetic simulations.

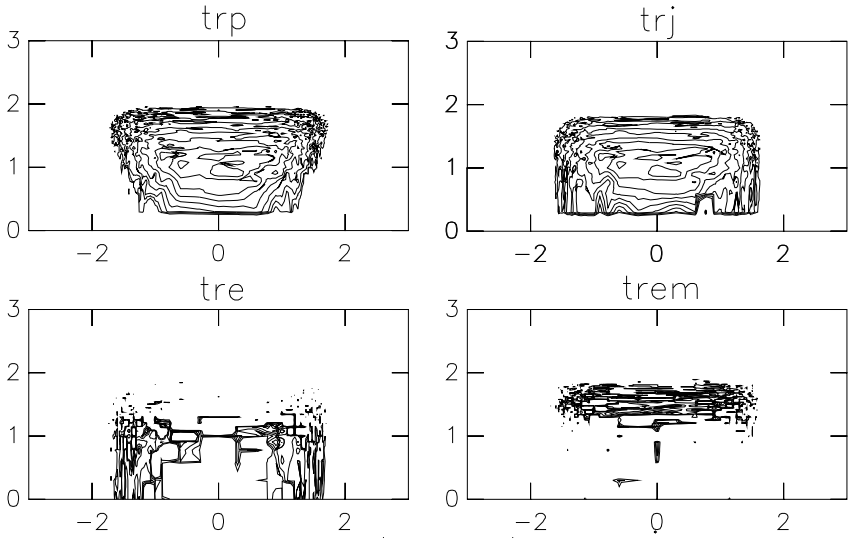

FIG. 3. $\mathbf{E} \times \mathbf{B}$ energy transfer rates in $(k_x \rho_s, k_y \rho_s)$ space on a logarithmic scale. Positive and negative contributions to Tr_e, denoted by "tre" and "trem", are shown separately.

On the role of zonal flows and fields. Zonal flows and fields are purely radial ($k_\theta = k_\parallel = 0$) variations of $\tilde{\phi}$ and $\tilde{A}_\parallel$ associated with $\mathbf{E} \times \mathbf{B}$ flows and magnetic field fluctuations. [12,13] They can be self-generated by the turbulence and may in turn act as its dominant nonlinear saturation mechanism. But how important are they on ρ_e scales? A typical snapshot of the flux-surface averaged values of $\tilde{\phi}$ and $\tilde{A}_\parallel$ as a function of the radial coordinate x (normalized to ρ_e) from a stellarator simulation (see Ref. [10]) is shown in Fig. 4 together with the $\mathbf{E} \times \mathbf{B}$ shearing rate $\tilde{\Omega} \equiv \tilde{v}'_{Ey}$ (in units of v_{te}/R) where the prime stands for d/dx. In this case, the space and time averaged RMS values of $\tilde{\Omega}$ and and the magnetic shear fluctuation, $\tilde{s} \equiv qR\tilde{B}'_y/B$, are given by $\tilde{\Omega}^{\mathrm{rms}} \approx 0.12\, v_{te}/R \sim 0.3\, \gamma^{\mathrm{max}}$ and $\tilde{s}^{\mathrm{rms}} \approx 0.018$ where γ^{max} is the maximum linear growth rate. This is in stark contrast to results from ITG turbulence where $\tilde{\Omega}$ can significantly exceed γ^{max} (e.g., $\tilde{\Omega}^{\mathrm{max}}/\gamma^{\mathrm{max}} \sim 14$ in Ref. [14]). In the ITG case, one obtains the zonal flow saturation criterion $\tilde{\Omega}^{\mathrm{rms}} \lesssim \gamma^{\mathrm{max}}$ only after correcting for the ineffectiveness of the high frequency component of $\tilde{\Omega}$. Moreover, the zonal components of ETG turbulence contribute only 1% or so to the total $\tilde{\phi}^{\mathrm{rms}}$. [10] This is again in contrast to the findings in the ITG case where zonal modes with $k_x \rho_i \sim 0.1$ tend to contribute significantly or even dominate the fluctuation free energy contained in $\tilde{\phi}$ (see, e.g., Ref. [14] and references therein).

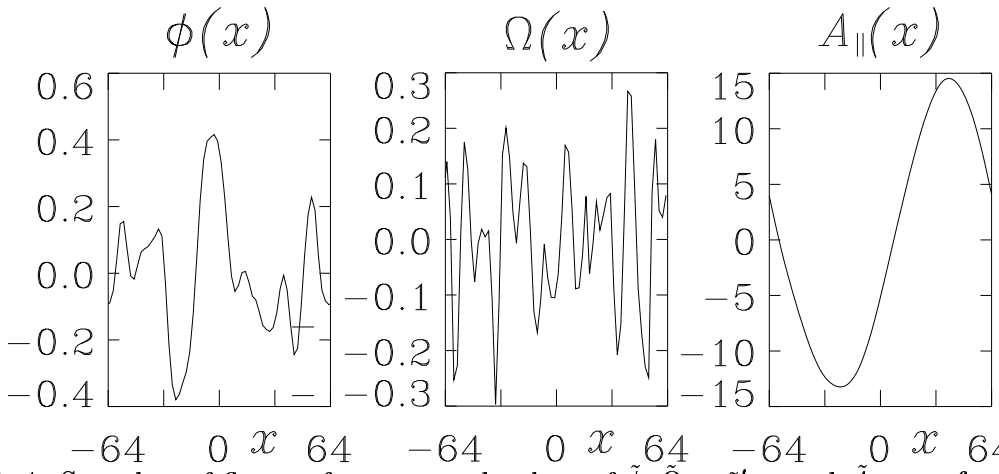

FIG. 4. Snapshot of flux surface averaged values of $\tilde{\phi}$, $\tilde{\Omega} \equiv \tilde{v}'_{Ey}$, and $\tilde{A}_\parallel$ as a function of the radial coordinate x.

It is well known that low-amplitude ITG streamers are broken up by zonal flows. [15] In the ETG case, however, the self-generated zonal flows are too weak (about 15-20 times weaker than in the ITG case as we have shown above) to break up the high-amplitude streamers. Moreover, since magnetic shear variations primarily affect the linear growth rates of the ETG modes driving the turbulence, [16] a value of $\tilde{s}^{\rm rms} \approx 0.018$ is certainly too small for zonal fields to play a significant role. Similar zonal flow/field saturation levels as the ones reported here have also been found in ETG simulations of tokamak plasmas. Thus, we may conclude that, at least for a significant region in parameter space, zonal modes on ρ_e scales tend to play a subdominant role in the turbulent dynamics. (A possible exception could be the simulation for tokamak edge parameters described in Ref. [8].) Here, it may be worth noting that many of the spectral properties of zonal modes are observed to be quite universal, indicating that a generic theory of zonal modes at hyperfine scales might be constructable on the basis of cascade physics. [10]

A predictive numerical model for turbulent transport. Building on these results on linear streamers, secondary instabilities, and zonal modes, we now develop an *ab initio* numerical model which is shown to even quantitatively explain the nonlinear gyrokinetic simulation results. [2] The application of secondary instability theory of course presupposes that the back reaction of zonal flows and fields on the turbulence can be ignored. As we have just seen, this is generally the case on ETG scales.

The basic idea is to predict the saturation amplitude by balancing primary (γ_ℓ) and

secondary ($\gamma_{\rm nl}$) growth rates. To do this, one must first calculate $\gamma_{\rm nl}$. At sufficiently high amplitude, $\gamma_{\rm nl} \propto \tilde{\phi}_\ell$. We thus compute $\gamma^0_{\rm nl}$ by freezing a given linear eigenmode at a fiducial high amplitude ($\tilde{\phi}_\ell = \tilde{\phi}^0_\ell$), and using this state as the "equilibrium" for a sequence of initial value calculations with varying k_x. (In the sequel, we consider $k_x/k_y = 0.5$ as a representative value.) Given $\tilde{\phi}^0_\ell$, $\gamma^0_{\rm nl}$ and γ_ℓ, the RMS amplitude of $\tilde{\phi}$ in the turbulent state is estimated by $\tilde{\phi}/\tilde{\phi}^0 = \gamma_\ell/\gamma^0_{\rm nl}$. (We note that all our results are in the strong turbulence regime, where $\chi_e \propto \tilde{\phi}$, so that $\gamma_\ell/\gamma^0_{\rm nl}$ also roughly predicts the anomalous transport coefficient.)

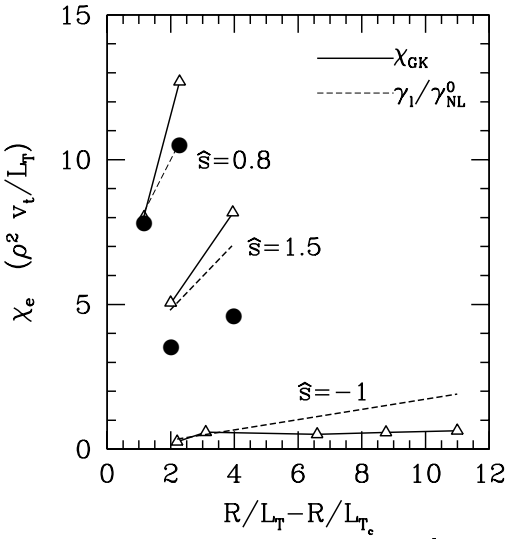

FIG. 5. χ_e from nonlinear gyrokinetic ETG simulations [open triangles] for our nominal parameters and $\hat{s} = 0.8$ ($R/L_{T_c} \sim 4.6$), $\hat{s} = 1.5$ ($R/L_{T_c} \sim 7.1$), and $\hat{s} = -1$ ($R/L_{T_c} \sim 6.3$), together with numerical [dashed lines] and semi-analytical [full circles] predictions.

Somewhat surprisingly, we find that ETG driven turbulent transport is well described by this relatively simple model as can be seen in Fig. 5. Here, the following physical parameters have been used (besides the ones mentioned in the figure itself): $R/L_n = 2.2$, $q = 1.4$, and $T_{i0}/T_{e0} = 1$, corresponding to the "Cyclone base case". A single fit parameter (related to the α_3 parameter in Section III and representing the ratio of the normalized heat flux to the normalized $\tilde{\phi}$) was held fixed for all the points in the figure. Importantly, neither the linear growth rate nor the maximal value of $\gamma/\langle k^2_\perp \rangle$ predicts the variation found in the nonlinear simulations. For example, the negative shear cases with $R/L_{Te} - R/L_{Tc} > 6$ have maximized $\gamma/\langle k^2_\perp \rangle$ values which *exceed* those of the $\hat{s} = 0.8$ cases. It is the variation of the secondary growth rate as the linear eigenfunction changes in response to the equilibrium parameters that correlates

with the difference in the nonlinear flux. The secondary growth rates exhibit a strong dependence on magnetic shear as the secondary transitions from a Rogers secondary (moderate positive shear) to a Cowley secondary (negative shear). The good agreement between gyrokinetic simulation and numerical model encourages us to persue a semi-analytical treatment of the balance between primaries and secondaries, condensing several important pieces of information about the saturated nonlinear state into into simple algebraic formulas.

III. TOWARDS AN ANALYTIC THEORY OF ∇T DRIVEN TURBULENCE

In the present Section, we restrict to $\hat{s} \gtrsim 0.4$ and $R/L_n \lesssim R/L_{T_j} \gg R/L_{T_j}^{\rm crit}$. In this parameter regime, ITG/ETG modes have a predominantly toroidal character and the Rogers secondary is the dominant nonlinear saturation mechanism. The region close to criticality (algebraic expressions for $R/L_{T_j}^{\rm crit}$ in tokamaks and the stellarator Wendelstein 7-AS have been derived in Refs. [17] and [9], respectively) as well as the low/negative shear region involve the Cowley secondary and are more difficult to treat. This task is left for future work. Using a host of linear gyrokinetic simulations, we find that under these conditions the linear growth rates of long-wavelength ITG/ETG streamers may be well described by the simple algebraic formula

$$\gamma_\ell = \frac{\alpha_1}{\tau_j}\,\frac{v_{tj}}{L_{T_j}}\,(k_\theta \rho_j - k_\theta^{\rm c}\rho_j)\,, \quad k_\theta^{\rm c}\rho_j = \frac{L_{T_j}}{qR}\,\tau_j^{1/2}\,, \quad \alpha_1 \approx 0.25\,. \tag{6}$$

Here, j labels ions and electrons (in the ITG and ETG case, respectively), and $\tau_e = T_{e0}/T_{i0} = 1/\tau_i$. Finite β and λ_{De} effects have again been neglected. Low k_θ tails due to kinetic effects have also been ignored since the corresponding streamers exhibit a clear slab-like parallel mode structure and are therefore expected to be strongly suppressed by Cowley secondaries. Eq. (6) states that beyond a certain threshold, γ_ℓ rises linearly with k_θ for $k_\theta \rho_j \ll 1$. Note that Eq. (6) is independent of $\hat{s}$ and R/L_n. Interestingly, this result can also be derived in the framework of gyrofluid theory. Employing, e.g., the basic model described by Eqs. (1-3) in Ref. [18], and generalizing their Eq. (3) to

$$\frac{\partial T}{\partial t} + A\,\nabla_\parallel v + \mu A\,|\nabla_\parallel| T = 0 \tag{7}$$

one gets exactly the above result with $\alpha_1 = 2\mu/(1+4\mu^2)$. Using $\mu = (8/\pi)^{1/2}$ as suggested by Hammett *et al.* [19] leads to the prediction $\alpha_1 \approx 0.285$ which is very close

to the gyrokinetic result. The cutoff wavenumber $k_\theta^{\rm c}$ may be interpreted as the perpendicular length scale at which the parallel transit frequency exceeds the diamagnetic frequency. Apparently, the detailed nature of the onset is determined by the quality of the Landau resonance model.

The second ingredient in our ETG/ITG turbulence theory is an algebraic formula for the nonlinear growth rates of Rogers secondaries in the presence of a large amplitude linear streamer. (Here, we will focus on the ETG case, the ITG case can be treated in an analogous fashion.) According to Fig. 4 in Ref. [4], its maximum with respect to k_x is given by

$$\gamma_{\rm nl} = \frac{\alpha_2}{\tau_e}\,\frac{v_{te}}{L_{T_e}}\,(k_\theta\rho_e)^4\left[\frac{e\tilde{\phi}}{T_e}\frac{L_{T_e}}{\rho_e}\right] \tag{8}$$

with $\alpha_2 \approx 0.18$. For $\hat{s} \neq 0$, the primary modes twist with the field lines, leading to an increase of the effective k_θ. We will take this effect into account by replacing k_θ^4 in Eq. (8) with $\langle k_\theta^2\rangle^2$ where the angular brackets denote weighting with $|\tilde{\phi}(\theta)|^2$,

$$\langle k_\theta^2\rangle = \int k_\theta(\theta)^2|\tilde{\phi}(\theta)|^2 d\theta \Big/ \int |\tilde{\phi}(\theta)|^2 d\theta = k_\theta^2\left(1+\hat{s}^2\langle\theta^2\rangle\right). \tag{9}$$

The gyrokinetic simulations show that the parallel mode structure is typically very well described by a Gaussian, such that we have $|\tilde{\phi}(\theta)|^2 \propto \exp(-\nu\theta^2)$ and consequently $\langle\theta^2\rangle = (2\nu)^{-1}$. A good fit formula for ν, inferred from dozens of linear gyrokinetic simulations for $\hat{s} \gtrsim 0.2$ and $R/L_{T_e} \gg R/L_{T_e}^{\rm crit}$, is

$$\nu = 0.53\,q\,(k_\theta\rho_e) + \max\{0.09, 0.19\,\hat{s}^2\}\,(q/\tau_e)\,(R/L_{T_e})\,(k_\theta\rho_e)^2\,. \tag{10}$$

Having established analytical expressions for the growth rates of primaries and secondaries, we can now explicitly balance the two,

$$\gamma_\ell = \gamma_{\rm nl}\,. \tag{11}$$

In the strong turbulence regime, this yields

$$\chi_e = \alpha_3\left[\frac{e\tilde{\phi}}{T_e}\frac{L_{T_e}}{\rho_e}\right]\frac{\rho_e^2 v_{te}}{L_{T_e}} = \frac{\alpha_1\alpha_3}{\alpha_2}\left[\frac{k_\theta - k_\theta^{\rm c}}{k_\theta^4}\right]\left[\frac{1}{1+\hat{s}^2/2\nu}\right]^2\frac{\rho_e^2 v_{te}}{L_{T_e}}\,. \tag{12}$$

Maximizing this expression over k_θ, using

$$\left[\frac{k_\theta - k_\theta^{\rm c}}{k_\theta^4}\right]_{\rm max} \approx 0.1055\,(k_\theta^{\rm c})^{-3} \quad \text{at} \quad k_\theta = 4k_\theta^{\rm c}/3 \equiv k_\theta^d\,, \tag{13}$$

one finally obtains

$$\chi_e = \frac{0.15}{\tau_e^{3/2}\,(1+\hat{s}^2/2\hat{\nu})^2}\left(\frac{qR}{L_{T_e}}\right)^3 \frac{\rho_e^2 v_{te}}{L_{T_e}} \tag{14}$$

where we have chosen $\alpha_3 = 1$ (in line with our nonlinear simulation results) and defined $\hat{\nu} = \nu(k_\theta = k_\theta^d)$. For sufficiently large temperature gradients, this can be written as

$$\chi_e \approx \mathcal{F}(q, \hat{s}, \tau_e)\,\frac{R}{L_{T_e}}\,\frac{\rho_e^2 v_{te}}{L_{T_e}}\,. \tag{15}$$

Evaluating this expression for the four points with positive shear shown in Fig. 5, we get surprisingly good agreement. Note that another prediction of this semi-analytical model is that the poloidal length scale of the dominant modes is given by k_θ^d. For Cyclone base case parameters (including $\hat{s} = 0.8$) we get $k_\theta^d \sim 0.13$, in reasonable accordance with nonlinear simulation results, exhibiting $k_\theta^d = 0.15 \pm 0.05$. [1,2]

An analogous treatment of ITG modes and associated Rogers secondaries leads to

$$\chi_i \approx \mathcal{G}(q, \hat{s}, \tau_i)\,\frac{\rho_i^2 v_{ti}}{L_{T_i}} \tag{16}$$

which is one order down in R/L_T compared to the ETG case, Eq. (15). A scaling like this has indeed been observed in nonlinear simulations of ITG turbulence with adiabatic electrons. [20] Moreover, the prediction $\mathcal{G}(q = 1.4, \hat{s} = 0.8, \tau_i = 1) \sim 2$ is roughly consistent with the simulation results. It should be kept in mind, however, that in contrast to the ETG case, ITG turbulence can be controlled by zonal modes, an effect which is not accounted for by the present theory. This is true, in particular, as the system approaches marginality.

IV. SUMMARY

Gyrokinetic simulations of ETG and ITG turbulence show that the linear symmetry between them is nonlinearly broken. This finding can be explained in terms of a secondary instability theory which may also serve as a basis for simple numerical or semi-analytical models. The latter are shown to successfully capture key features of the streamer-dominated turbulent state even quantitatively. This raises hope that more comprehensive analytical theories of temperature gradient driven turbulence might be

developed along those lines. On the other hand, it shows that the standard interpretation of turbulent transport as some type of isotropic diffusion (random walk) process is not universally applicable. While the mixing length estimate of the transport level induced by curvature-driven turbulence, $\chi \sim \gamma^{\max}/k_\theta^2 \sim \rho^2 v_t/L_T$, does a reasonable job for ITG modes, it fails completely in the ETG case.

---

[1] F. Jenko, W. Dorland, M. Kotschenreuther, and B. N. Rogers, Phys. Plasmas **7**, 1904 (2000).

[2] F. Jenko and W. Dorland, *Prediction of significant tokamak turbulence at electron gyroradius scales*, submitted to Phys. Rev. Lett.

[3] S. C. Cowley, R. M. Kulsrud, and R. Sudan, Phys. Fluids B **3**, 2767 (1991).

[4] W. Dorland, F. Jenko, M. Kotschenreuther, and B. N. Rogers, Phys. Rev. Lett. **85**, 5579 (2000).

[5] T. Antonsen and B. Lane, Phys. Fluids **23**, 1205 (1980).

[6] E. A. Frieman and L. Chen, Phys. Fluids **25**, 502 (1982).

[7] M. A. Beer, S. C. Cowley, and G. W. Hammett, Phys. Plasmas **2**, 2687 (1995).

[8] F. Jenko and W. Dorland, Plasma Phys. Control. Fusion **43**, A141 (2001).

[9] F. Jenko and A. Kendl, New Journal of Physics **4**, 35 (2002).

[10] F. Jenko and A. Kendl, *Radial and zonal modes in hyperfine-scale stellerator turbulence*, to appear in Phys. Plasmas.

[11] B. Scott, New Journal of Physics **4**, 52 (2002).

[12] A. Hasegawa and M. Wakatani, Phys. Rev. Lett. **59**, 1581 (1987).

[13] P. N. Guzdar, R. G. Kleva, A. Das, and P. K. Kaw, Phys. Rev. Lett. **87**, 015001 (2001).

[14] T. S. Hahm, M. A. Beer, Z. Lin *et al.*, Phys. Plasmas **6**, 922 (1999).

[15] Z. Lin, T. S. Hahm, W. W. Lee *et al.*, Science **281**, 1835 (1998).

[16] C. Holland and P. H. Diamond, *Electromagnetic secondary instabilities in electron temperature gradient turbulence*, to appear in Phys. Plasmas.

[17] F. Jenko, W. Dorland, and G. W. Hammett, Phys. Plasmas **8**, 4096 (2001).

[18] M. Ottaviani, M. A. Beer, S. C. Cowley *et al.*, Phys. Rep. **283**, 121 (1997).

[19] G. W. Hammett, W. Dorland, and F. W. Perkins, Phys. Fluids B **4**, 2052 (1992).

[20] A. M. Dimits, G. Bateman, M. A. Beer *et al.*, Phys. Plasmas **7**, 969 (2000).